Inorg. Chem. **2004**, *43*, 50–56

Lead Tetrakis(imidazolyl)borate Solids: Anion Exchange, Solvent Intercalation, and Self Assembly of an Organic Anion

Barton H. Hamilton, Kathryn A. Kelly, Todd A. Wagler, Matthew P. Espe, and Christopher J. Ziegler*

Department of Chemistry, Knight Chemical Laboratory, University of Akron, Akron, Ohio 44325-3601

Received September 23, 2003

The coordination polymer $Pb[B(Im)_4](NO_3)(xH_2O)$, constructed by using sodium tetrakis(imidazolyl)borate and lead(II) nitrate solutions, is a layered material with the metal centers facing the interlayer spacing. As in naturally occurring layered minerals, this compound can readily undergo anion exchange and reversible intercalation of solvent water in the solid state with retention of crystallinity. We observed changes in solvent intercalation by ^{207}Pb solid state NMR (SSNMR) and thermogravimetric analysis (TGA). Stoichiometric exchange of ^{15}N nitrate for nitrate and iodide for nitrate is monitored by ^{15}N and ^{207}Pb SSNMR, and single crystals of the iodide-exchanged material $Pb[B(Im)_4]I$ were isolated. While the iodide compound can be obtained through facile exchange from the nitrate parent compound, the organic anion benzoate is placed in the interlayer spacing for nitrate under self-assembly conditions and forms an alternating monolayer in $Pb[B(Im)_4](C_6H_5COO)(0.5H_2O)$. The ion exchange versus self-assembly behavior correlates with the structural differences in the three compounds. In both $Pb[B(Im)_4]I$ and $Pb[B(Im)_4](C_6H_5COO)(0.5H_2O)$, the lead sites act as Lewis acids for the iodide and benzoate, respectively.

Introduction

As the field of crystal design has grown over the past decade, synthetic efforts are being directed toward constructing functional solids.[1] Coordination polymers are attractive targets for crystal design since one can design two aspects of the solid: the identity of the metal ion[2] and the structure of the linking ligand unit.[3] These two components of a coordination polymer can have a direct impact on its functionality; the metal ion can provide a site for reactivity within the solid, and the organic ligand can help control the topology of the network solid. In particular, network solids with Lewis acidic metals remain an area of focus in crystal engineering.[4]

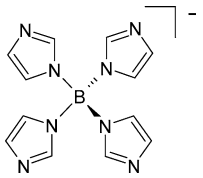

Figure 1. Tetrakis(imidazolyl)borate.

We are investigating the coordinating anion tetrakis(imidazolyl)borate ($B(Im)_4^-$, Figure 1) as a component of coordination solids.[5] This species is a robust, multidentate ligand that is readily synthesized from simple starting materials.[6] The tetrahedral geometry about the boron in $B(Im)_4^-$ is structurally rigid and promotes the formation of three-dimensional structures in coordination solids. In addition, the anion can be readily modified to explore the effects of functionalization on network structure. Finally, the anionic nature of tetrasubstituted boron can provide charge balance for the metals in coordination polymers.

* To whom correspondence should be addressed. E-mail: ziegler@uakron.edu.

(1) (a) Rosi, N. L.; Eckert, J.; Eddaoudi, M.; Vodak, D. T.; Kim, J.; O'Keeffe, M.; Yaghi, O. M. *Science* **2003**, *300*, 1127−1129. (b) Jiang, H.; Hu, A.; Lin, W. *Chem. Commun.* **2003**, 96−97. (c) Lee, S. J.; Hu, A.; Lin, W. *J. Am. Chem. Soc.* **2002**, *124*, 12948−12949. (d) Janiak, C.; Scharmann, T. G.; Albrecht, P.; Marlow, F.; Macdonald, R. *J. Am. Chem. Soc.* **1996**, *118*, 6307−6308.

(2) (a) Hamilton, B. H.; Ziegler, C. J. *Chem. Commun.* **2002**, 842−843. (b) Harrison, R. G.; Fox, O. D.; Meng, M. O.; Dalley, N. K.; Barbour, L. J. *Inorg. Chem.* **2002**, *41*, 838−843.

(3) (a) Moulton, B.; Zaworotko, M. J. *Chem. Rev.* **2001**, *101*, 1629−1658. (b) Eddaoudi, M.; Moler, D. B.; Li, H. L.; Chen, B.; Reineke, T. M.; O'Keeffe, M.; Yaghi, O. M. *Acc. Chem. Res.* **2001**, *34*, 319−330.

(4) (a) Noro, S.; Kitagawa, S.; Yamashita, M.; Wada, T. *Chem. Commun.* **2002**, 222−223 (b) Li, H.; Davis, C. E.; Groy, T. L.; Kelley, D. G.; Yaghi, O. M. *J. Am. Chem. Soc.* **1998**, *120*, 2186−2187.

(5) Hamilton, B. H.; Kelly, K. A.; Malasi, W.; Ziegler, C. J. *Inorg. Chem.* **2003**, *42*, 3067−3073.

(6) (a) Trofimenko, S. *J. Am. Chem. Soc.* **1967**, *89*, 3170−3177. (b) Trofimenko, S. *J. Coord. Chem.* **1972**, *2*, 75−77. (c) Chao, S.; Moore, C. M. *Anal. Chim. Acta* **1978**, *100*, 457−467.

10.1021/ic035117d CCC: $27.50
Published on Web 12/11/2003

In this report, we present a series of compounds that incorporate $B(Im)_4^-$ in a coordination polymer with Pb^{2+}. We have recently presented part of this work as a Communication.[7] These compounds have the generic formula $Pb[B(Im)_4]X(nH_2O)$, where X is NO_3^- in the parent structure and *n* ranges from 0 to 1.5. The parent material, grown by diffusing solutions of $Pb(NO_3)_2$ and $Na[B(Im)_4]$, adopts a layered structure with noncoordinating nitrates found between the layers and the Pb ions facing the layer interface. This network solid, which resembles naturally occurring layered minerals, exhibits ion exchange behavior and water intercalation resulting from its tiered structure. Related materials of the formula $Pb[B(Im)_4]X(nH_2O)$, where $X = I^-$ or $C_6H_5COO^-$, are generated by ion exchange of the nitrates or by self-assembly, respectively. In both of the nitrate-substituted structures, the Pb^{2+} ion behaves as a Lewis acid, fulfilling an important criterion for functional coordination polymers. We have characterized these materials by X-ray structural elucidation, and their dynamic chemistry by using solid state NMR spectroscopy (SSNMR).

Experimental Section

All reagents and solvents were purchased from Aldrich and used as received. Water was purified by using a Milli-Q reagent water system. Elemental analysis was performed at the School of Chemical Sciences Microanalytical Laboratory at the University of Illinois at Urbana-Champaign. Infrared spectroscopy was carried out on a Bomem MB-100 IR system. Sodium tetrakis(imidazolyl)-borate was prepared as previously described.[6]

Solid State Nuclear Magnetic Resonance. Solid-state NMR spectra were obtained on a Varian Unityplus-200 (4.7 T) spectrometer using Doty Scientific supersonic and standard magic-angle spinning (MAS) probes. All spectra were collected with MAS and sample spinning speeds of 2.7−8 kHz. Samples were packed into 7 mm silicon nitride rotors with Kel-F end caps. ^{15}N (20.5 MHz) Bloch decay spectra were acquired using a 200 s relaxation delay and a spinning speed of 2.7 kHz. ^{207}Pb (42.2 MHz) spectra were acquired using a Hahn-echo sequence with a 5 s relaxation delay and a spinning speed of 5−8 kHz. ^{15}N and ^{207}Pb chemical shifts were referenced to solid $^{15}NH_4{}^{15}NO_3$ ($\delta_{NH4} = 0$ ppm) and 0.5 M $Pb(NO_3)_2$ ($\delta_{Pb} = -2941$ ppm) as external references, respectively. A 55 kHz decoupling field strength was used in all experiments. Isotropic chemical shifts in the ^{207}Pb spectra were determined by collecting the spectra at several sample spinning speeds.

Synthesis of $Pb[B(Im)_4](NO_3)(xH_2O)$ ($x = 0-1.5$) (1). A solution of $Pb(NO_3)_2$ (331 mg, 1.0 mmol) in 10 mL deionized water was added to a 1:1 ethanol/water solution (10 mL) of sodium tetrakis(imidazolyl)borate (302 mg, 1.0 mmol). A white, microcrystalline precipitate of $Pb[B(Im)_4](NO_3)(xH_2O)$ formed immediately and was collected by filtration. Yield: 469 mg (82%). Large crystals of $Pb[B(Im)_4](NO_3)(xH_2O)$ were grown by slow diffusion of layers of the above two solutions at 60 °C. Anal. Calcd for $C_{12}H_{12}BN_9O_3Pb$ (dried) (%): C, 26.2; H, 2.1; N, 22.3. Found: C, 26.33; H, 1.85; N, 22.84. IR (KBr): 3468, 3080, 1631, 1478, 1420, 1384, 1294, 1249, 1214, 1108, 1082, 1034, 1006, 940, 928, 816, 766, 663 cm^{-1}. ^{13}C SSNMR: 143, 131, 123 ppm.

Synthesis of $Pb[B(Im)_4]I$ (2). Crystals of $Pb[B(Im)_4](NO_3)(xH_2O)$ (200 mg, 0.35 mmol) were suspended in a 10 mL aqueous solution of 1 equiv of NaI (51 mg, 0.35 mmol) and gently agitated for 24 h. Crystals of $Pb[B(Im)_4]I$ were washed with water, collected by filtration, and air-dried. The yield was quantitative (110 mg). Anal. Calcd for $C_{12}H_{12}BN_8IPb$ (%): C, 23.5; H, 1.9; N, 18.3. Found: C, 23.4; H, 1.80; N, 18.08. IR (KBr): 3467, 3080, 1484, 1475, 1299, 1247, 1212, 1106, 1081, 1037, 940, 928, 816, 762, 663 cm^{-1}. ^{13}C SSNMR: 148, 141, 131, 128, 124, 122 ppm.

Synthesis of $Pb[B(Im)_4](C_6H_5COO)(0.5H_2O)$ (3). $Pb(NO_3)_2$ (218 mg, 0.67 mmol) was dissolved in 4 mL of deionized water and placed at the bottom of a narrow test tube. A solution was made of a 3-fold excess of sodium benzoate (290 mg, 2.0 mmol) and 1 equiv of sodium tetrakis(imidazolyl)borate (205 mg, 0.67 mmol) in 4 mL of deionized water which was buffered with nitric acid to pH ∼ 7.0. The benzoate/borate solution was carefully layered on top of the lead(II) solution, and the tube sealed and placed in an oven at 60 °C for 3 days. White, needlelike crystals of $Pb[B(Im)_4](C_6H_5COO)(0.5H_2O)$ were collected by filtration. Yield: 302 mg (70%). Anal. Calcd for $C_{19}H_{18}BN_8O_{2.5}Pb$ (%): C, 37.0; H, 2.9; N, 18.1. Found: C, 36.61; H, 2.01; N, 17.58. IR (KBr): 3440, 3128, 1592, 1508, 1490, 1386, 1303, 1266, 1254, 1246, 1212, 1107, 1081, 1024, 936, 922, 851, 817, 754, 712, 683, 660 cm^{-1}. ^{13}C SSNMR: 174, 143, 141, 139, 133, 130, 122 ppm.

Table 1. Crystallographic Data Collection and Structure Parameters for Compounds **1**−**3**

	1	**2**	**3**
mol formula	$C_{12}H_{14.70}BN_9O_{4.35}Pb$	$C_{12}H_{12}BIN_8Pb$	$C_{19}H_{18}BN_8O_{2.50}Pb$
fw	572.18	613.20	616.41
space group	$P\bar{1}$	$P\bar{1}$	$P\bar{1}$
a, Å	8.5337(8)	8.5459(16)	8.6848(10)
b, Å	10.7463(9)	10.0336(19)	8.7774(10)
c, Å	11.2476(10)	10.965(2)	14.1567(16)
α (deg)	74.6840(10)	102.070(3)	80.382(2)
β (deg)	79.2840(10)	104.408(3)	81.598(2)
γ (deg)	67.0120(10)	103.875(3)	78.860(2)
Z	2	2	2
V (Å^3)	911.84(14)	847.2(3)	1036.7(2)
T (°C)	−173	−173	−173
λ (Å)	0.71073	0.71073	0.71073
abs coeff μ_{calc} (cm^{-1})	0.9293	1.1789	0.8175
δ_{calc} (Mg/m^3)	2.084	2.404	1.971
$R(F_o)^a$	0.0371	0.0511	0.0275
$R_w(F_o^2)^b$	0.0721	0.1000	0.0640

$^a R = \sum||F_o| - |F_c||/\sum|F_o|$. $^b R_w = [\sum w(|F_o^2| - |F_c^2| - |F_c^2|)^2/\sum w(F_o^2)^2]^{1/2}$.

X-ray Crystallography. The X-ray intensity data for compounds **1**−**3** were measured at 100 K (Bruker KRYO−FLEX) on a Bruker SMART APEX CCD-based X-ray diffractometer system equipped with a Mo-target X-ray tube ($\lambda = 0.71073$ Å). The crystals were mounted on cryoloops using Paratone N-Exxon oil and placed under a stream of nitrogen. The detector was placed at a distance of 5.009 cm from the crystal. Frames were collected with a scan width of 0.3° in *ω*. The frames for each data set were integrated with the Bruker SAINT software package using a narrow-frame integration algorithm. The data were corrected for absorption with the SADABS program. The structure was solved and refined using the Bruker SHELXTL (Version 6.1) Software Package until the final anisotropic full-matrix least-squares refinement on F^2 converged.[8] Experimental details for the three structures are shown in Table 1

$^{15}NO_3^-$ Anion Exchange Experiments. A 300 mg sample of $Pb[B(Im)_4](NO_3)(1.35\ H_2O)$ was gently agitated in a 10 mL solution

(7) Hamilton, B. H.; Kelly, K. A.; Wagler, T. A.; Espe, M. P.; Ziegler, C. J. *Inorg. Chem.* **2002**, *41*, 4984−4986.

(8) Sheldrick, G. M. *SHELXTL, Crystallographic Software Package*, version 6.10; Bruker-AXS: Madison, WI, 2000.

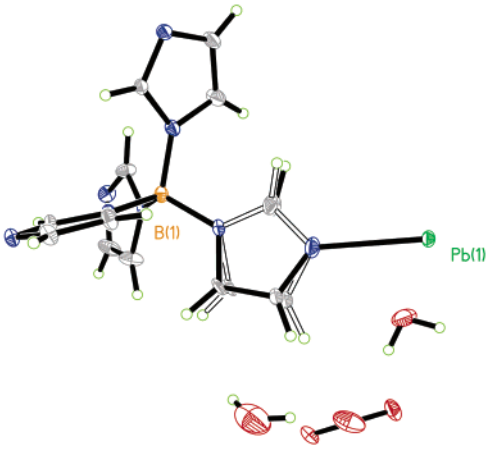

Figure 2. The asymmetric unit of $Pb[B(Im)_4](NO_3)(H_2O)_{1.35}$.

of 1 equiv $Na^{15}NO_3$ for 24 h. The resultant exchanged crystals were then collected in quantitative yield. ^{15}N SSNMR spectra were taken of the sample prior to exchange, immediately after exchange, and after washing the exchanged sample with distilled H_2O.

Thermogravometric Analysis. Thermogravametric analysis was measured on a TA instruments 2050 device. The TGA measurements of compounds **1**, **2**, and **3** were carried out over a temperature range 25−600 °C at a scan rate of 10°/min.

Results and Discussion

The reaction of a H_2O/EtOH solution of $Na[B(Im)_4]$ and aqueous $Pb(NO_3)_2$ produces a product with the formula $Pb[B(Im)_4](NO_3)(nH_2O)$, where $n = 0-1.5$. If the solutions are mixed together quickly, a microcrystalline product is produced, whereas slow diffusion of layered, equimolar solutions results in large, single, platelike crystals. The crystalline product is resilient to most organic solvents and water and desiccates rapidly upon exposure to dry air. The single crystals are suitable for X-ray structural elucidation. The repeating asymmetric unit of the crystal structure with 50% thermal ellipsoids is shown in Figure 2. One imidazole ring is linked to the metal center in this unit, and each of the remaining heterocycles is linked to different lead sites in adjacent asymmetric units. The nitrate anion, required for charge balance, and the water molecules occupy the void space in the unit.

In the extended network, the Pb−borate units link together to form a layered solid, shown in Figure 3. Each metal is coordinated by four imidazole rings from different borates, although this is not obvious from the figure due to the overlapping perspective of the imidazole rings. The nitrates and solvent water molecules occupy the spacing between the Pb−borate tiers. The metal sites face the interlayer spacing, and the borates transverse the layer itself. The distance between Pb sites across the layer interface (based on the mean planes of the Pb centers) is ∼3.4 Å, although the edges of the peripheral imidazole rings extend slightly further into the interlayer spacing. The borate−Pb layer is ∼6.3 Å across using the same measurement convention.

Table 2. Selected Bond Lengths and Angles for Compounds **1**−**3**

	1	**2**	**3**
Pb−N (Å)	2.406(3)	2.381(7)	2.396(3)
	2.505(3)	2.531(6)	2.575(3)
	2.523(4)	2.594(7)	2.717(3)
	2.643(3)	2.615(6)	2.776(3)
Pb−X (Å)		3.1507(7) (Pb−I)	2.478(3) (Pb−O)
			2.542(3) (Pb−O)
N−Pb−N (deg)	77.09(12)	76.4(2)	72.69(10)
	78.30(10)	76.6(2)	76.46(10)
	79.03(11	79.0(2)	77.60(10)
	80.66(12)	82.3(2)	79.08(10)
	83.86(11)	93.8(2)	82.84(11)
	149.58(11)	155.3(2)	146.87(10)

The environment around the metal sites in this solid is asymmetric and described as a hemidirected Pb center.[9] Figure 4 shows the coordination environment about each Pb ion in the network solid, and Table 2 lists bond lengths and angles about the metal center. The geometry at the Pb centers conforms to the VSEPR prediction of a disphenoidal system with a stereochemically active lone pair in an equatorial position directed toward the layer interface. There are no other bonding interactions in the vicinity of the metal; the nitrates and the water molecules are not bound, and the closest distance between metal centers is ∼4.4 Å, which is much too long to be a bonding contact. The Pb sites in this solid are coordinatively unsaturated since the large radii of Pb can typically accommodate up to 8 ligands.[9] The presence of a lone pair as well as a low coordination number indicates that the metal sites in this solid could be amphoteric. We have observed the Lewis acidity of this solid upon replacement of the nitrate with a coordinating anion, which will be described below.

In addition, the layered structure of $Pb[B(Im)_4](NO_3)$ suggests chemistry akin to that found in minerals with a similar topology.[10] Layered minerals, such as clays and

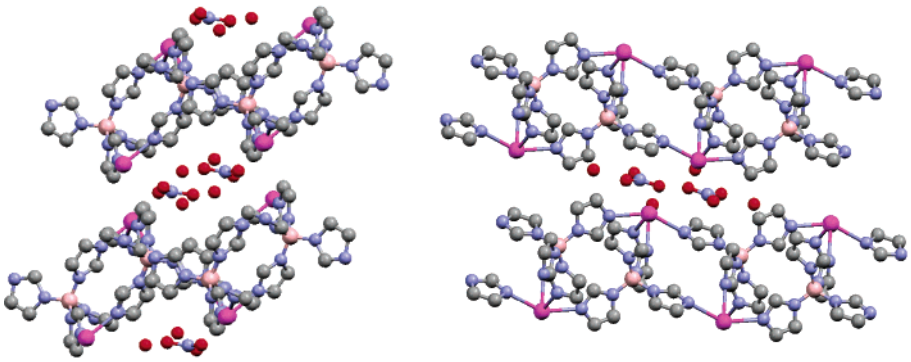

Figure 3. Extended structure of $Pb(B(Im)_4)(NO_3)(H_2O)_{1.35}$ along the *c* axis (a) and *a* axis (b). The lead atoms are in purple, and hydrogen atoms have been omitted for clarity.

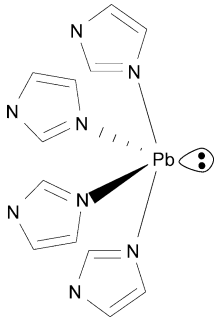

Figure 4. The coordination environment about the metal center in Pb[B(Im)$_4$](NO$_3$). The geometry is a distorted disphenoid, with the VSEPR predicted lone pair directed toward the layer interface.

hydrotalcites, can intercalate neutral guests, exchange ions, and catalyze reactions in the interlayer spacing. We investigated this topology-related chemistry in Pb[B(Im)$_4$](NO$_3$), focusing on intercalation chemistry and anion exchange. A number of coordination polymers exhibit both types of reactivity, which can be considered a measure of the potential usefulness of a network structure. For example, coordination solids that preferentially sequester certain anions could be used to treat wastewater contaminated with negatively charged toxic or radioactive species.[11]

The intercalation and ion exchange chemistry of these layered materials is readily monitored by using solid state NMR (SSNMR). The effect of intercalation and/or exchange on the Pb environment was investigated by using ^{207}Pb SSNMR, as this isotope is ideal for NMR studies: 23% natural abundance, $I = {}^1/_2$, and a chemical shift range encompassing almost 8000 ppm that is very sensitive to changes in its local environment.[12] The ^{207}Pb spectrum from the parent compound is shown in Figure 5a where the isotropic chemical shift is −533 ppm, and the chemical shift anisotropy covers ∼2500 ppm. As the spectrum was obtained by using a single excitation pulse (Bloch decay) with the RF frequency near the isotropic chemical shift, the intensities of the spinning sidebands nearer the edges of the spectrum are reduced in intensity from their actual values. However, this perturbation of the peak intensities does not affect the interpretation of the ^{207}Pb NMR data. The coordination environment and network connectivity of Pb[B(Im)$_4$](NO$_3$) is similar to the litharge form of PbO;[13] however, the ^{207}Pb chemical shift of litharge is +2000 ppm. The differences in the chemical shifts result in part from the substitution of nitrogen for oxygen in Pb[B(Im)$_4$](NO$_3$) as the coordinating atoms despite the similarities between the two solids.[14,15] The

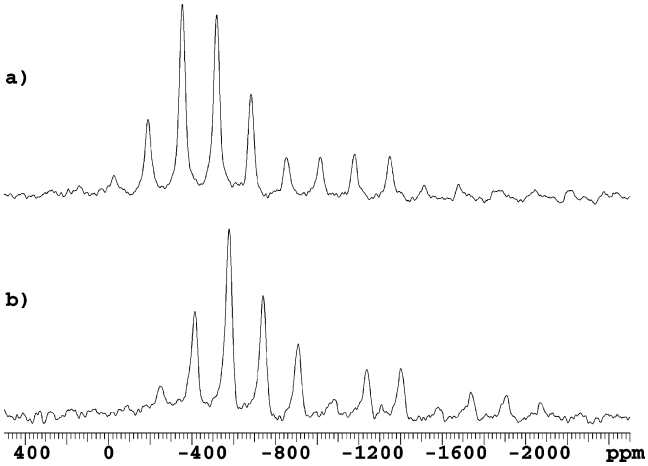

Figure 5. ^{207}Pb SSNMR of Pb[B(Im)$_4$](NO$_3$)(H$_2$O)$_x$ under 99% humidity (a) and 24% humidity (b). TGA measurements indicate that $x = 1.5$ and 0.25 for (a) and (b), respectively.

^{207}Pb spectrum (Figure 5a) consists of a single set of peaks indicating only one Pb environment in the material. Also, the relatively narrow line widths indicate a homogeneous local environment at each Pb site. These results are consistent with the single crystal XRD studies of the parent compound discussed above.

Crystals of Pb[B(Im)$_4$](NO$_3$)(nH$_2$O) desiccate rapidly upon exposure to dry air, eventually resulting in Pb[B(Im)$_4$](NO$_3$). The material can also be rehydrated without significant loss in crystallinity, indicative of the reversible intercalation of solvent water molecules. The extent of hydration and the effect of the presence of water at the Pb site was monitored by SSNMR. Two ^{207}Pb SSNMR spectra from a slightly dry (equilibrated in 24% humidity at 25 °C) and a water saturated sample (equilibrated in 99% humidity at 25 °C) of Pb[B(Im)$_4$](NO$_3$) are shown in Figure 5. The structures of both spectra are similar but shift by ∼50 ppm downfield from the partially dry sample (0.25 water molecules per unit) to the water saturated sample (1.5 solvent water molecules per unit). We confirmed the number of water molecules per asymmetric unit by TGA. The ∼50 ppm shift is relatively small on the ^{207}Pb chemical shift range and is indicative of a change in solvation only and not the coordination environment of the metal.

We began our investigation of anion exchange by replacing the nitrate in solid Pb[B(Im)$_4$](NO$_3$) for labeled nitrate and monitoring by ^{15}N SSNMR under magic angle spinning conditions.[7] The initial ^{15}N spectrum of Pb[B(Im)$_4$](NO$_3$) prior to exposure shows no signal (Figure 6a). We were able to replace some of the NO_3^- in the solid with $^{15}NO_3^-$ by exposing crystals to an aqueous solution with a mole equivalent of Na^{15}NO$_3$. After collecting the crystals by filtration, the material was again characterized by ^{15}N SSNMR. Prior to washing, the ^{15}N NMR spectrum contains two peaks at 355.4 and 353.2 ppm. This was reduced to a single peak at 353.2 ppm when the crystals were washed several additional times with water (Figure 6b). Comparison

(9) Shimoni-Livny, L.; Glusker, J. P.; Bock, C. W. *Inorg. Chem.* **1998**, *37*, 1853−1867.
(10) Cheetam, A. K.; Day, P. *Solid State Chemistry*; Clarendon Press: Oxford, 1992.
(11) (a) Lagadic, I. L.; Mitchell, M. K.; Payne, B. D. *Environ. Sci. Technol.* **2001**, *35*, 984−990. (b) Nash, K.; Fried, S.; Friedman, A. M.; Sullivan, J. C. *Environ. Sci. Technol.* **1981**, *15*, 834−837. (c) Wang, P.; Anderko, A.; Turner, D. R. *Ind. Eng. Chem. Res.* **2001**, *40*, 4444−4455.
(12) (a) Kim, K. S.; Bray, P. J. *J. Magn. Reson.* **1974**, *16*, 334−338. (b) Piette, L. H.; Weaver, H. E. *J. Chem. Phys.* **1958**, *28*, 735−736.
(13) Fayon, F.; Farnan, I.; Bessada, C.; Coutures, J.; Massiot, D.; Coutures, J. P. *J. Am. Chem. Soc.* **1997**, *119*, 6837−6843.
(14) Curtis, R. D.; Hilborn, J. W.; Wu, G.; Lumsden, M. D.; Wasylishen, R. E.; Pincock, J. A. *J. Phys. Chem.* **1993**, *97*, 1856−1861.
(15) (a) Vassilev, P.; Nihtianova, D. *Acta Crystallogr., Sect. C* **1998**, *54*, 1062−1064. (b) Greenwood, N. N.; Earnshaw, A. *Chemistry of the Elements*; Pergamon Press: Oxford, 1984.

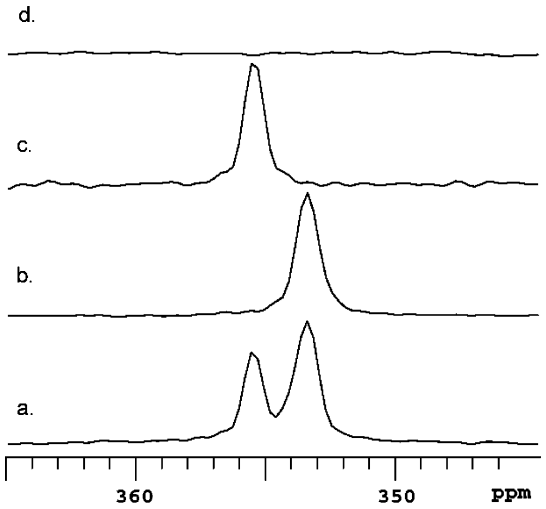

Figure 6. ^{15}N SSNMR spectra of (a) Pb[B(Im)$_4$](NO$_3$) after exposure to aqueous Na^{15}NO$_3$, (b) washed Pb[B(Im)$_4$](Na^{15}NO$_3$) after exchange, (c) Na^{15}NO$_3$, and (d) Pb[B(Im)$_4$]I. The spinning speed was 2.7 kHz.

with the ^{15}N NMR spectrum from solid Na^{15}NO$_3$ reveals that the peak at 355.4 ppm arises from adventitiously bound Na^{15}NO$_3$ (Figure 6c); thus, the peak at 353.2 ppm results from the intercalated nitrate ions.

We also expected that Pb[B(Im)$_4$](NO$_3$) should show a preference for soft anions due to the presence of the lead ions at the layer interface. We can monitor the replacement of nitrate for iodide by using the above $^{15}NO_3^-$ exchanged sample. The solid sample containing $^{15}NO_3^-$ was exposed to a mole equivalent solution of KI, collected, washed with water, and again examined by ^{15}N SSNMR. The peak at 353.2 ppm is absent (Figure 6d), showing that iodide exchange has occurred replacing the nitrate anion in the layered material. Complete exchange takes place with iodide at stoichiometric concentrations. During both of the exchange interactions, the crystallinity of the material was not greatly affected; some loss of crystal size occurs depending on the vigor of stirring during the exchange process. Powder XRD patterns of Pb[B(Im)$_4$](NO$_3$) both before and after exchange with $^{15}NO_3^-$ and I^- show no change in the degree of crystallinity, although the pattern does change upon exchange with I^-, as expected. In addition, IR spectra of Pb[B(Im)$_4$](NO$_3$) before and after exchange with I^- show the same fingerprint except for the loss of a peak at 1385 cm^{-1} that corresponds to a strongly absorbing nitrate vibration. Finally, CHN elemental analysis is in complete agreement with the complete exchange of iodide for nitrate.

The effect of the exchange of iodide for nitrate on the Pb site was also characterized by ^{207}Pb SSNMR. The spectrum of the starting material prior to exchange, Pb[B(Im)$_4$](NO$_3$), is shown in Figure 7a. Upon substituting I^- for NO_3^-, the ^{207}Pb spectrum changes in both chemical shift and line width, as shown in Figure 7c. The ^{207}Pb chemical shift moves downfield to 357 ppm, a result of perturbation of the electron distribution at the Pb. The magnitude of this shift (~900 ppm) is much larger than the shift observed upon changing the water solvation of the Pb site (~50 ppm). However, the chemical shift change is also relatively small compared to the complete range of shifts observed for Pb (~8000 ppm).

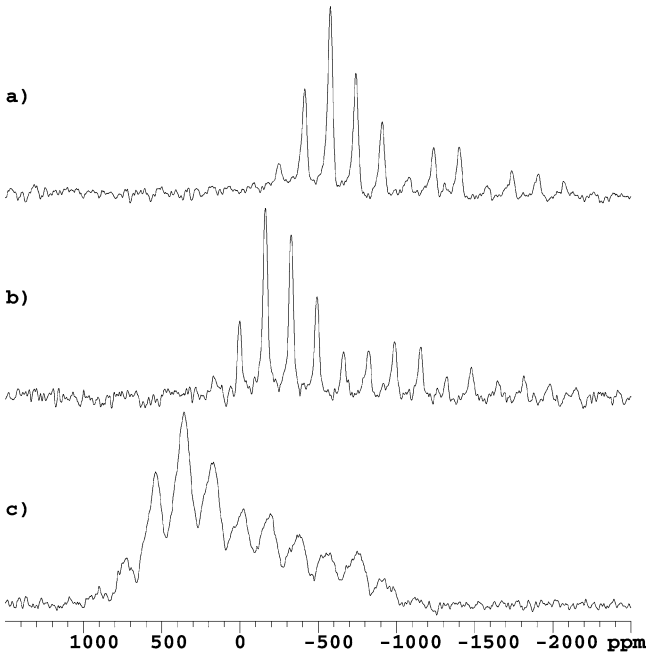

Figure 7. ^{207}Pb SSNMR spectra of (a) Pb[B(Im$_4$)](NO$_3$)(0.25H$_2$O), (b) Pb[B(Im)$_4$](O$_2$CC$_6$H$_5$), and (c) Pb[B(Im$_4$)]I. The spinning speed was 8 kHz.

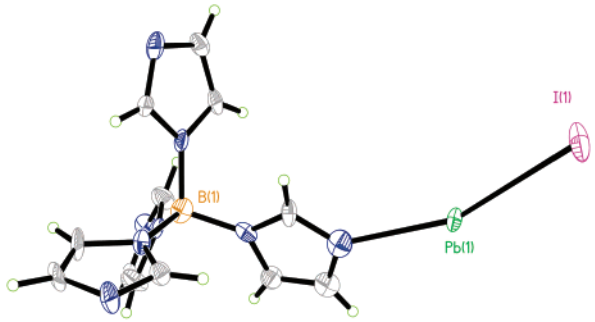

Figure 8. The asymmetric unit with 50% thermal ellipsoids of Pb[B(Im)$_4$]I.

This change in chemical shift indicates that there is a direct interaction between the iodide and the metal, but the Pb-[B(Im)$_4$] structure has not been significantly changed. The NMR results are in agreement with the aforementioned powder XRD and IR experiments that also indicated a small change in the Pb coordination.

We were able to characterize the nature of this lead−iodide interaction by isolation of a single crystal from the exchange reaction. Figure 8 shows the structure of the asymmetric unit of Pb[B(Im)$_4$]I, and Figure 9 shows its extended network structure. As in the starting material, the borate−metal ratio remains the same, but the noncoordinating nitrate and water molecules have been replaced with the iodide. The metal center acts as a Lewis acid upon exchange with iodide, forming a Pb−I bond of 3.1507(7) Å. The mean distance for Pb(II)−I bonds for structures found in the Cambridge Structural Database (CSD) has an average value of 3.22(16) Å, and the bond length found in Pb[B(Im)$_4$]I is in good agreement with this number.[9] In the iodide exchanged material, the formation of this bond has the net effect of eliminating some of the void space in the asymmetric unit. The cell volume reduces from 911.84(14) Å^3 in the nitrate compound to 847.2(3) Å^3 in Pb[B(Im)$_4$]I. This bond also

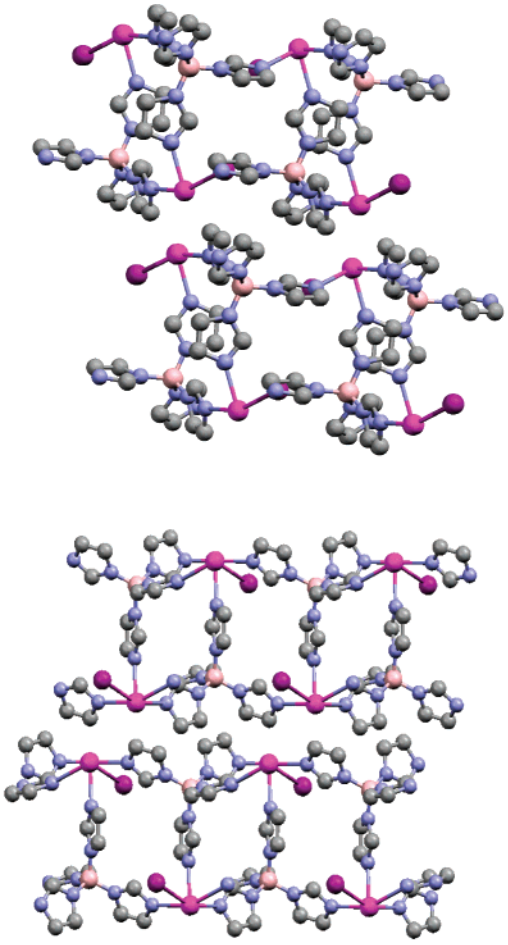

Figure 9. Extended structure of $Pb(B(Im)_4)I$ along the *b* axis (a) and *a* axis (b). The hydrogen atoms have been omitted for clarity.

increases the coordination number from four to five, but the metal center still retains a hemidirected geometry.

In the extended network structure of $Pb[B(Im)_4]I$, the Pb−borate connectivity remains the same as that in the parent network $Pb[B(Im)_4](NO_3)$, and the Pb ions still face the interlayer spacing. Upon examination of the extended structure, the change in asymmetric unit volume becomes more apparent. The Pb−I bond does not extend into the interlayer spacing, but the ordinate of the bond is directed roughly parallel to the layer itself. This effective elimination of the anion from the interlayer spacing allows the layers to pack more closely together than in the parent $Pb[B(Im)_4](NO_3)$ structure. The spacing decreases from ∼3.4 Å between planes of the Pb atoms in the nitrate compound to a length of only ∼3.0 Å in the iodide exchanged material.

The formation of a lead iodide bond in $Pb[B(Im)_4]I$ upon exchange does not affect the metal−nitrogen bond lengths despite the modification of the geometry, as shown in Table 2. The average Pb−N bond lengths in $Pb[B(Im)_4]I$ and $Pb[B(Im)_4](NO_3)$ both equal ∼2.53 Å. In addition, the N−Pb−N angles do not significantly shift upon the binding of iodide to the metal, changing by only a few degrees. The similarity of the bond lengths and angles both before and after exchange explain in part how crystallinity is retained upon iodide exchange.

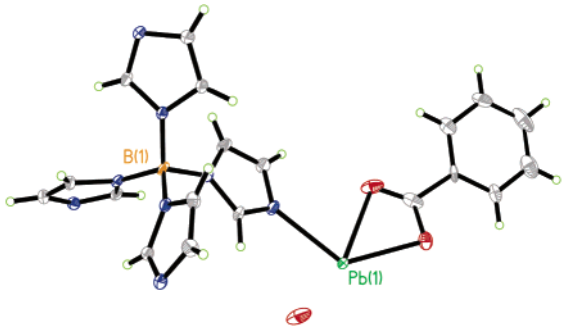

Figure 10. The asymmetric unit with 50% thermal ellipsoids of $Pb[B(Im)_4](O_2C_7H_5)(0.5H_2O)$ The hydrogens on the solvent water molecule are not shown, and only one of two orientations of the disordered benzoate is shown.

We also explored exchange with the organic anion benzoate but found that we were unable to replace the nitrate using conditions similar to those for iodide. However, we did find that by growing crystals of $Pb[B(Im)_4](NO_3)$ in the presence of a 3:1 mole excess of an aqueous, buffered solution of benzoate, we were able to obtain $Pb[B(Im)_4](O_2C_7H_5)(0.5H_2O)$. In this case, unlike the iodide exchange, the material clearly forms by self assembly. We characterized this material by X-ray crystallography, and the asymmetric unit is shown in Figure 10 with the extended network structure shown in Figure 11. As in the iodide exchanged structure, the stoichiometry and the connectivity of the lead−borate units are identical to that of the parent $Pb[B(Im)_4](NO_3)$. The benzoate replaces the nitrate as the counterion and coordinates to the metal center in a symmetric bidentate fashion. While the coordination of iodide to the lead center decreases the volume of the asymmetric unit, the presence of the benzoate, a much larger anion, increases the cell volume significantly to 1036.7(2) $Å^3$.

The extended network structure of $Pb[B(Im)_4](O_2C_7H_5)(0.5H_2O)$ shows the same layered arrangement as observed in both $Pb[B(Im)_4]I$ and $Pb[B(Im)_4](NO_3)$. The benzoates occupy the interlayer spacing and arrange in an alternating monolayer. The presence of this monolayer significantly increases the spacing between the lead−borate tiers to a length of 5.99 Å between planes of the Pb atoms. Upon examination of the Pb−N bonds and the geometry around the metal center in $Pb[B(Im)_4](O_2C_7H_5)(0.5\ H_2O)$, there are some changes relative to the parent $Pb[B(Im)_4](NO_3)$ structure. The coordination of the benzoate has a larger effect on the Pb−N bond lengths, which increase to an average of ∼2.62 Å. However, as in $Pb[B(Im)_4]I$, the N−Pb−N bond angles do not change much upon substitution of the organic anion. The Pb−O bonds in $Pb[B(Im)_4](O_2C_7H_5)(0.5\ H_2O)$ are similar to those observed for other structures with coordinated oxygens; we observe an average Pb−O bond length of ∼2.51 Å compared to an average of 2.53(15) Å from the CSD.[9]

The ^{207}Pb SSNMR spectrum of $Pb[B(Im)_4](O_2C_7H_5)(0.5\ H_2O)$ shows a change in chemical shift relative to the parent compound. As can be seen in Figure 7b, the chemical shift of $Pb[B(Im)_4](O_2C_7H_5)(0.5H_2O)$ lies between those of the nitrate and iodide compounds, exhibiting the change to the Pb environment as one goes from the noncoordinating nitrate

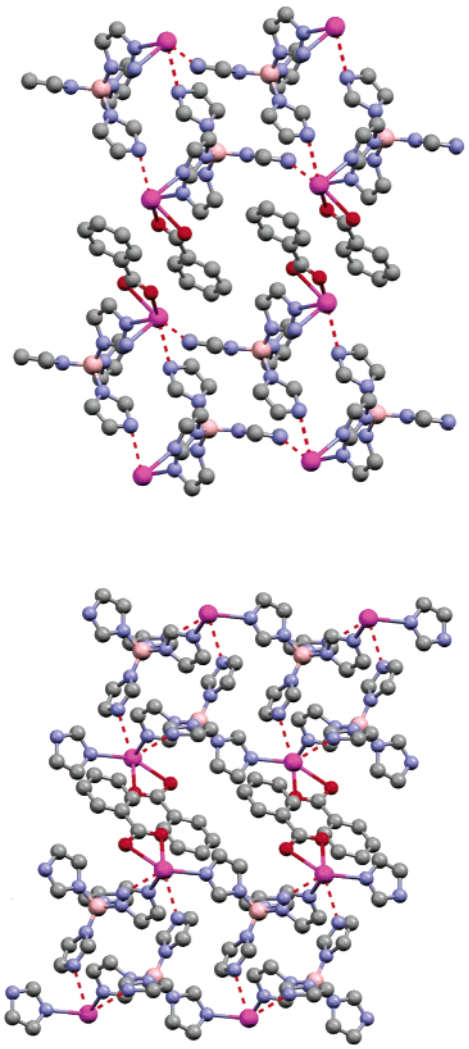

Figure 11. The layered network structure of $Pb[B(Im)_4](O_2C_7H_5)(0.5\ H_2O)$ viewed along the *b* axis (a) and the *a* axis (b). The solid lines about the metal ions indicate short coordination bonds (<2.6 Å), and the dashed lines indicate longer coordination bonds (>2.7 Å). Hydrogen atoms and the solvent water have been omitted for clarity.

to the weak coordination of the carboxylate and the strong coordination of the iodide. Interestingly, the ^{207}Pb SSNMR spectrum of the benzoate substituted material is close to that of the water-saturated nitrate material (Figure 5a). In the case of both the benzoate and water-saturated $Pb[B(Im)_4](NO_3)$, there are oxygen atoms close or bound to the metal center, which most likely governs the observed chemical shifts.

The difference (or lack thereof) in the lead coordination environment upon ligand binding may explain why iodide exchange can occur with retention of crystallinity. Since the bond lengths and angles do not significantly change upon substitution with iodide, the exchange of this anion could occur without disruption of the crystalline lattice. In addition, there is only a small change in the volume of the unit cell upon iodide exchange (~60 $Å^3$, a 7% change). In contrast, replacing the nitrate with a benzoate imparts larger changes on the network structure. The bond lengths distort more than upon iodide exchange, and the volume of the unit cell increases by 13%. These differences may explain why $Pb[B(Im)_4](O_2C_7H_5)(0.5H_2O)$ only forms by self-assembly.

The ability to replace the nitrate in $Pb[B(Im)_4](NO_3)$ with other anions bodes well for its potential use as a scaffold for advanced materials. We are currently investigating the incorporation of other organic and inorganic anions between layers of $Pb[B(Im)_4]^+$. In addition to examining the fundamental anion exchange chemistry of $Pb[B(Im)_4]^+$ layered solids, we intend to incorporate guests with specific physical or chemical attributes. We anticipate that functional guest molecules will impart their properties onto the material.

Acknowledgment. C.J.Z. acknowledges the University of Akron for faculty research grants (FRG-1524 and FRG-1565). We also wish acknowledge NSF Grant CHE-0116041 for funds used to purchase the Bruker-Nonius diffractometer and the Kresge Foundation and donors to the Kresge Challenge Program at The University of Akron for funds used to purchase the NMR instrument used in this work.

Supporting Information Available: Thermogravametric analyses and crystallographic information files (CIF). This material is available free of charge via the Internet at http://pubs.acs.org.

IC035117D